Chapter 5

Performance Analysis of an Integrated Starter-Alternator-Booster for Hybrid Electric Vehicles

Florin-Nicolae Jurca and Mircea Ruba

Additional information is available at the end of the chapter

http://dx.doi.org/10.5772/intechopen.68861

Abstract

The chapter aims to investigate the reduction of the fuel consumption of conventional vehicles using mild-hybridization and considering the New European Driving Cycle (NEDC), using two topologies of electrical machines dedicated to integrated starter-alternator-booster (ISAB) applications: directly connected to the crankshaft (called 'normal ISAB') and indirectly through the belt system (called BSAB), respectively. The behaviour of ISAB and BSAB of a hybrid electric vehicle has been investigated with a multi-domain simulation software developed in Advanced Modelling Environment for performing Simulation (AMESim).

Keywords: electrification, hybrid electric vehicle, integrated starter-alternator-booster, electrical machine

1. Introduction

As the electrification of vehicle propulsion at low (e-bikes) and high power (buses) continues to extend, the current research efforts on this topic are focused especially on increasing the autonomy of vehicles due to the accumulation of electricity. Due to the lack of charging station and low autonomy in terms of maintaining a reduced weight of the battery, the electrical vehicle is momently limited to urban trails. In this context, the hybrid electric vehicles (HEVs) were considered initially as a transition between conventional vehicles (internal combustion engine (ICE)) and the electric ones, and now they still remain a viable solution that is gaining ground by combining the advantages of both types of vehicles [1–4].

The trend in all types of vehicles (conventional, electrical, or hybrid vehicles) for the next years is to increase the equipment with different types of electrical subsystems. These can be related

to the safety (direction, breaking, lights, distance sensors, mirrors etc.) or to the comfort (seats, HAVC, audio, navigation display etc.). At the same time, a lot of traditional mechanically driven loads are replaced with electrical driven ones (water pumps, servo steering, ventilation fan, etc.). This demand of electrical energy, of around 10 kW [5], requires increasing generator power and a certain level of efficiency (normally situated at 40–55%) [6]. A common alternator in a car is relatively cheap and with low efficiency, but with the expected increase of power, it exceeds the capability of the Lundell generator (claw pole synchronous machine). In this context, the replacement of classical alternator with a high efficiency machine is mandatory. Besides this, the operating mode of the conventional starter (around 1 s for each start) is used only for the start of the ICE and after it becomes an extra weight in the vehicle. The easy (costs and implementation) solution of this problem is to replace both machines (starter and alternator) with a single electrical machine.

The initial concept of the integrated starter-alternator (ISA) system was developed in order to gain more space for the powertrain system and to reduce the weight of the vehicle by combining the starter with the alternator. This system ensures the start/stop of the internal combustion engine and the supply with electricity of all the auxiliary subsystems (safety or comfort).

Especially in parallel configuration of HEV, the ISA is used for starting the internal combustion and supply the electrical load. A second electrical machine is necessary for the electric propulsion. The method for the simplification of this structure involves the use of a single electric machine comprising three operating modes: starter-alternator and booster. In this case, the integrated starter-alternator-booster (ISAB) system will be able initially to start the ICE, then, when it is turned on, it will reverse to generator mode and will supply electricity to consumers and the storage system. By adopting adequate control strategies, the electrical machine is capable of moving quickly from generator to motor (booster) and back in order to help the international combustion engine for a short period of time (maximum 2–3 min), if more power is necessary (overruns, ramp, curbs, etc.) [7]. This operating mode of the machine is generically called integrated starter-alternator-booster (ISAB). Using ISAB in parallel HEV is generically called *Mild-HEV*. In this configuration, the full electric propulsion of the vehicle is not possible, but the production costs necessary for the implementation of the hybridization in conventional vehicles are lowest compared to other variants of HEV.

According to Ref. [8], where the influence of fuel consumption for a small car equipped with ISAB is investigated and considering the European standard (1999/100 EC), the fuel consumption is reduced to about 12% in total.

The increase in the number of electric components within the vehicles boosts the market for electrical motors for hybrid and electric vehicles. A Frost & Sullivan market research finds that the market earned revenues of about 55 million Euros in 2010, which are expected to reach $1.6 billion by the end of 2017 [9].

The required characteristics of the ISAB in the starter mode and alternator (generator) mode are very restrictive for a conventional electrical machine [10]:

- High value of electromagnetic torque for starting ICE (120–300 Nm).
- High efficiency at wide speed range (600–6000 rpm).
- Reliability at high vibrations and over 250,000 start/stop cycles (during 10 years).
- Operation at temperatures between −30 and 130°C.
- Easy maintenance and low cost and so on.

Usually, the ISAB can be connected with a gasoline or diesel engine, either directly through the crankshaft (see **Figure 1**) or indirectly through the belt system (see **Figure 2**); based on that, the systems are called belt-driven starter-alternator-booster (BSAB) and conventional ISAB, respectively.

The size of the electrical machine is very important for BSAB application in order to keep the overall size low (the same dimensions like the ones of a conventional alternator) but for a given maximum torque, the systems usually have a recommended gear ratio 3:1 to the ICE crankshaft, according to Ref. [8]. The BSAB runs with a speed three times higher than the ICE. For the ISAB, the speed range is usually synchronized with combustion engine.

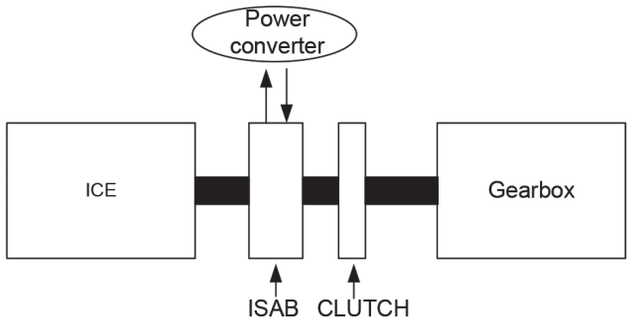

Figure 1. The ISAB system.

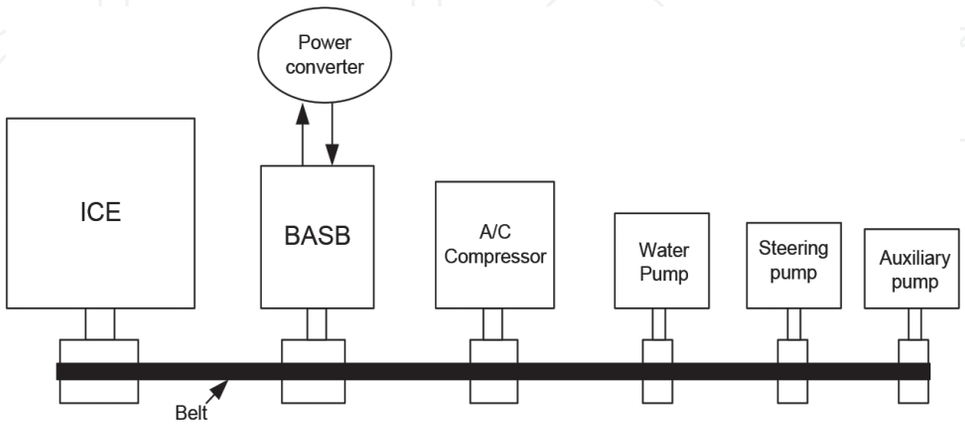

Figure 2. The BSAB system.

2. Electrical drive used for ISAB applications

2.1. Electrical machines

In the last decade, the development of power electronics (inverter/convertor) made the alternative current (AC) machines the best solution for ISAB applications, especially due to their high power density. These are synchronous reluctance machine (SynRM), induction machine and permanent magnet synchronous machines (PMSM) in both supplying variants: with sinusoidal and trapezoidal current.

The detailed investigation of SRM and induction machine is presented in Refs. [11, 12]. In these studies, the complicated electronics needed for SRM and the difficult control of the induction machine (influence of slip in performance of the machine) are highlighted. In this context, the SynRM and PMSM are the best candidates for ISAB applications.

The electrical machines used for conventional ISAB applications are exposed at high temperatures generated by ICE. This makes impossible the use of the PMSM in high efficiency and low-cost conditions (only with a special method for cooling or using expensive SmCo magnet). Therefore, the SynRM without permanent magnets is the best solution for the direct connection to the crankshaft of ICE (ISAB) and PMSM machine for BSAB.

2.1.1. PMSM machine for BSAB applications

The main advantage of the PMSM compared with other types of electrical machine is their high efficiency due to the absence of the field coil losses. The stator is constructed from three-phase windings and steel sheets (the same as the induction machine), but due to the absence of iron losses, the rotor is built from massive steel and permanent magnets. The position of the permanent magnets can be categorized as surface-mounted type and interior type. This position can have a significant effect on the mechanical and electrical characteristics, especially on the synchronous inductance [13]. Because the permeability value of rare earth magnet (such as NdFeB) is very close to that of the air, the air gap of the machine with mounted surface PM effectively becomes larger in this case. This makes the machine *d*-axis inductance value very low, with a significant effect on the ability of overloading the machine and operation at flux weakening. Because the maximum torque is inverse proportional with the *d*-inductance, this becomes very large. But the low value of *d*-inductance reduces the possibility to operate at flux weakening. This is caused by the need to use a high value of the demagnetization component of the stator current in order to decrease the flux value in the air gap. Therefore, the remained current on the *q* axis will be insufficient to produce torque.

In the case of the interior magnets, it is possible to obtain a sinusoidal distribution of the air-gap flux by using simple rectangular magnets. A sinusoidal flux distribution reduces considerably the cogging torque, in particular in the case of the machine with a large number of pole pairs and a small number of slots per pole and phase [14]. For these structures, it is also possible to increase the flux density in the air gap beyond the value of the remnant flux density of the magnets by using the flux concentrators. Because in this case the *d*-inductance is usually higher than with that of the surface magnets topologies, the overload capacity of the machine will be reduced and the performance in flux weakening conditions will be higher.

http://dx.doi.org/10.5772/intechopen.68861

The PMSM with outer rotor (PMSMOR) (see **Figure 3**) is one of the special topologies of PMSM, with some advantages for BSAB applications:

- Belt mounted directly on the outer rotor, without using pulley.
- Easy mounting of permanent magnets, the centrifugal forces do not influence their mechanical stability.
- High torque capabilities.
- Convenience of cooling, etc.

The development cycle of PMSM (inner or outer rotor) topologies includes analytical procedure, magnetic field analysis and optimization procedure connected to previous design steps. The analytical procedure is presented in detail in Refs. [13, 14] and includes the following topics: analysis of the specifications, selection of the topology, the active and passive materials, sizing the machine, choice of the manufacturing technologies and information about preliminary cost evaluation. In the dimensioning procedure, classical formulas or dedicated software platforms like SPEED software can be used.

The electromagnetic flux analysis is realized with dedicated programs (like Flux 2D/3D, Jmag 2D/3D, Maxwell 2D/3D, ANSYS, Opera, open-source programs, etc.) based on the finite element method (FEM). The FEM is a widely used method for obtaining a numerical approximate solution for a given mathematical model of the machine. The obtained results are related to the voltage/current waveform, map of flux density, electromagnetic torque, losses (iron and Joule), and the efficiency value or map of it.

The optimization of electric machine is a multivariable, nonlinear problem with constraints. In order to treat problems with constraints, it is necessary to transform them into unconstrained ones. This can be done, for instance, by embedding the constraints in the objective function.

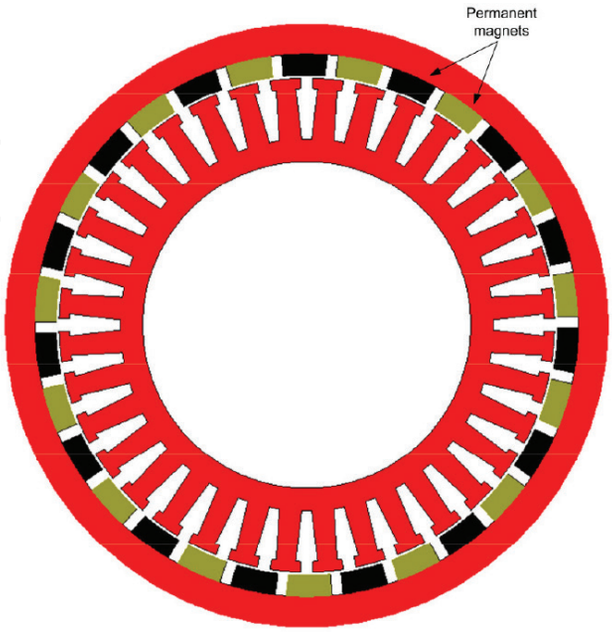

Figure 3. PMSMOR type.

The most used optimization algorithms in design of all types of electrical machines are as follows: genetics algorithms (GA), differential evolution algorithm (DEA), estimation of distribution algorithms (EDAs), particle swarm optimization (PSO) and multi-objective genetic algorithms (MOGA, Pareto, etc.) [15].

A comprehensive evaluation of optimization algorithms was performed in Refs. [16–18]. The authors of these studies state that any such classification of different optimization algorithms is not truly appropriate since the performance is an objective closely related to the specifics of each application. Nevertheless, in the optimization of the electrical machine, the authors mostly agree that DEA achieves the best fitness values, i.e. the minimum objective function value, usually with a smaller number of evaluation steps.

Considering the important step in the development of cycle of PMSM presented above, a general design procedure of PMSMOR for BSAB applications is proposed and presented in **Figure 4**.

2.1.2. SynRM machine for ISAB applications

Variable reluctance synchronous machines have received little attention in various comparative studies approaching the selection of the most appropriate electric-propulsion system for either HEV or EV. Malan [19, 20] showed that the SynRM drive has major advantages in electrical

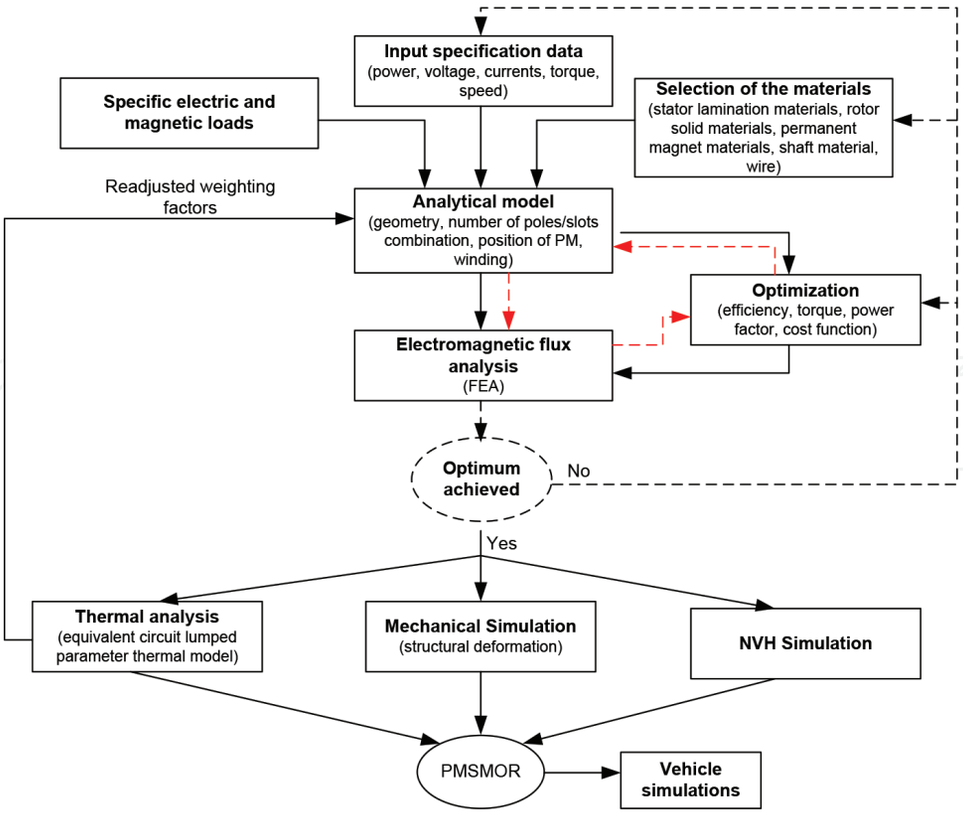

Figure 4. General design procedure of PMSMOR.

http://dx.doi.org/10.5772/intechopen.68861

propulsion. SynRM's performance strongly depends on the saliency ratio, but increasing the saliency complicates the rotor construction and drastically increases the motor cost. Interesting results concerning the influence of the saliency ratio on the SynRM steady-state performances, mainly on power factor and efficiency, are given in Ref. [21], while the effect of rotor dimensions on *d*- and *q*-axis inductances in the case of a SynRM with flux barrier rotor is discussed in Ref. [22]. Thus, the number of rotor flux barrier for the SynRM recommended in the literature is four. Above this value, the technology of the rotor is too complicated, while for a value lower than 4, the value of the torque ripple is too high. Regarding the rotor construction, there are three main different types, given in Ref. [23], presented in **Figure 5**.

- With salient rotor poles (see **Figure 5a**): require low technological effort and are obtained by removing the iron material from each rotor pole in the transversal region.
- With axially laminated rotor (ALA) (see **Figure 5b**): the rotor core is made of axial steel sheets that are insulated from each other using electrically and magnetically insulation (passive material).
- Transversally laminated anisotropic rotor (TLA) (see **Figure 5c**): the so-called ribs are obtained by punching and then the various rotor segments are connected to each other by these ribs.

The SynRM has a larger torque density compared with that of IM. This comes from the absence of rotor cage and related losses. A different dynamic behaviour is expected from SynRM due to the specific relationships between currents and fluxes. Because SynRM does not have a traditional cage (especially used for starting), it is necessary to use the modern inverter technology. Therefore, most of the literature on SynRM drives has concentrated mainly on the design and control of the machine with the goal of improving control, efficiency and torque production, drive flexibility and cost [24].

The main drawback of SynRM is related to structural behaviour at high speeds (over 10,000 rpm) because the specific geometry of the rotor involves thin layers of steel and large cut-off areas.

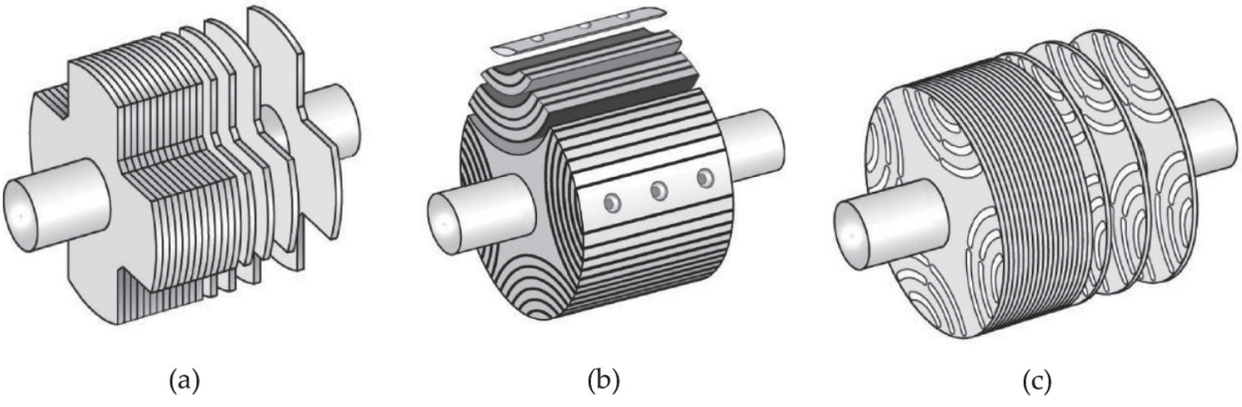

Figure 5. Rotor topologies for a SynRM: (a) simple salient pole, (b) axially laminated anisotropy rotor, and (c) transversally laminated anisotropic rotor. *Source*: [23].

Based on advantages and disadvantages of the SynRM and the specific applications of ISAB (rated speed up to 10,000 rpm), SynRM is one of the most suitable candidates for direct connection to crankshaft. The major advantages are high torque, thermal behaviour (absence of permanent magnets and low average value of iron losses), high value of efficiency at entire drive cycle of functioning, vibro-acoustic behaviour (low noise), etc.

In the development cycle of SynRM presented below, the most important step is related to the rotor geometry and the structural behaviour (see **Figure 6**).

2.2. Power electronics

The electrical equipment installed on the vehicles operates at a nominal voltage of 14 V. In the early 1990s, a new standard (PowerNET) for automotive electrical systems has been proposed by a consortium of automotive manufacturers (Daimler-Benz and General Motors). Following a proposal by the PowerNET, the voltage level increases for the electrical installation to 42 V [25]. The goal was to reduce the section of the conductors and gain the possibility to increase the total

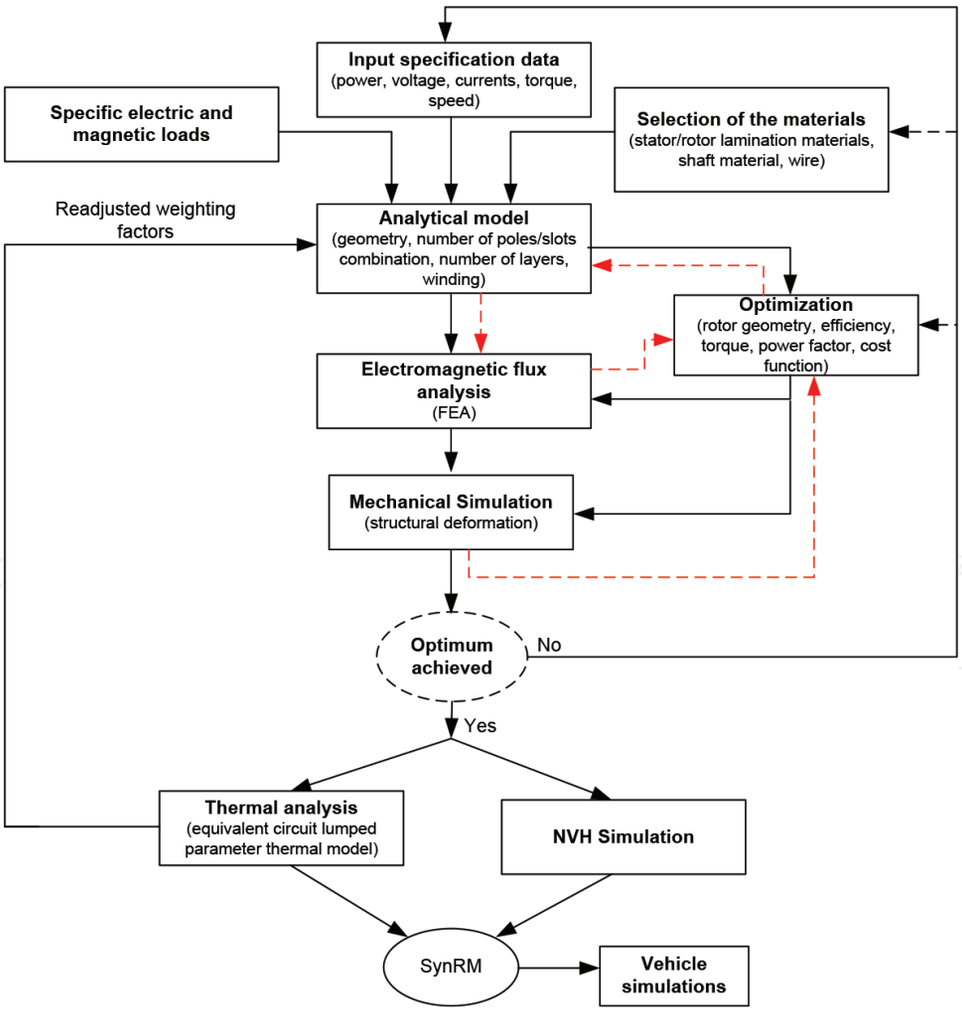

Figure 6. General design procedure of SynRM.

http://dx.doi.org/10.5772/intechopen.68861

power installed in the new generation of vehicle. The standard did not become very popular because of its high implementation costs, which would require the redesign of all electrical and electronical subsystems [26]. Instead, most producers were oriented on systems with two voltage levels: high voltage for propulsion and low voltage for auxiliary and electronic subsystems.

A starter-alternator system involves the use of a static frequency converter for the driving of the electrical machine. The convertor will operate in both the inverter and rectifier regimes. In the rectifier operating mode, it is indicated to adopt a control strategy of the converter with the purpose of reducing losses and the harmonic content of the output currents of the machine. The techniques for the control of the converter for these two modes are the same, only the current reverses its sense depending on the operating mode.

The input voltage of the static frequency converter is a DC voltage, the value of which must be kept constant in order to function optimally. The regulation of the input voltage of the converter can be done by using a bidirectional DC/DC converter with a closed loop control. An alternative to the use a DC/DC stage converter and another DC/AC converter is to use a Z-Source Converter [27]. The Z-Source Converter is more capable compared with the classical converter to operate both as a boost and buck converter due to the input impedances that give it particular operating properties.

2.2.1. Power electronics of SynRM and PMSM

For the control of PMSM machine, the current of the q axis is maintained maximum in order to produce high value of the torque and zero for d axis current, respectively. Instead, for SynRM, the control strategies mean to keep the equal value of the q axis current with the d axis. In the case of PMSM with interior magnets, this control strategy does not provide maximum torque due to the additional reluctant torque [28] component that appears in expression:

$$T = \frac{3}{2} \cdot p \cdot \left[\Psi_{\mathrm{PM}} \cdot i_q - (L_q - L_d) \cdot i_d \cdot i_q \right] \tag{1}$$

where T is the electromagnetic torque, p is a pair pole number, Ψ_{PM} is the permanent magnet flux, i_q is q axis current, i_d is d axis current, and L_q, L_d are q axis and d axis inductances.

The reluctant component of the torque has a maximum value for $i_d \neq 0$ and the stator current equal with $\pi/4$.

Usually, the implemented control method for the PMSM and SynRM for automotive application is an indirect method, which is based on measuring the stator currents and calculating the rotor flux phasor magnitude and position using these currents and the rotor position. Thus, the flux transducer or flux estimators that are usually used in the vector control method with direct measurement of flux are eliminated. This method has a disadvantage due to the fact that the accurate determination of rotor flux phasor position requires a precise measurement of rotor position. Thus, the practical implementation using speed measurement for obtaining the integration of the rotor angle is not recommended. Hence, an incremental encoder position or a resolver, which has a higher cost while providing the precision required of a vector control with a good dynamic response in applications is used. In addition to this vector control method that uses position sensors for determining the rotor angle control,

other methods where these transducers are eliminated (sensorless) exist. In these cases, the rotor position is estimated by using complex algorithms, using as input the measurement values of voltages and currents [29].

The general diagram control presented in **Figure 7**, usually used for PMSM and SynRM, can be divided into power and control components. The power circuit consists of the electrical machine (PMSM/SynRM), DC/DC converter, inverter, while the control loop consists of speed transducer, current transducers, PWM signal generation block, transformation of coordinate systems blocks and computing block of references current.

The control strategies considered for the SynRM are:

- Maximum torque control per ampere control (MPTAC)

The model of control is based on imposing the same currents for the d and q axes of the machine as current references for the vector control of the machine. These currents are calculated from the torque equation like

$$i_d = i_q = \sqrt{\frac{T_{\text{ref}}}{p \cdot (L_d - L_q)}} \tag{2}$$

- Maximum rate of change of torque control (MRCTC)

The control strategy is implemented in order to obtain fast machine response at sudden torque steps of the load. The idea here is to compute the d and q current component functions of some machine parameters and to use these components as input of the vector control scheme. The detailed control strategy is presented in Ref. [30].

- Maximum power factor control (MPFC)

The aim of this method is to maximize the power factor of the machine. For this, the d and q current components are computed as follows:

$$I_{q\text{imposed}} = T_{\text{ref}} \cdot \frac{1}{p} \cdot \frac{1}{L_d - L_q} \cdot \frac{1}{I_{d\,(\text{from the machine})}} \tag{3}$$

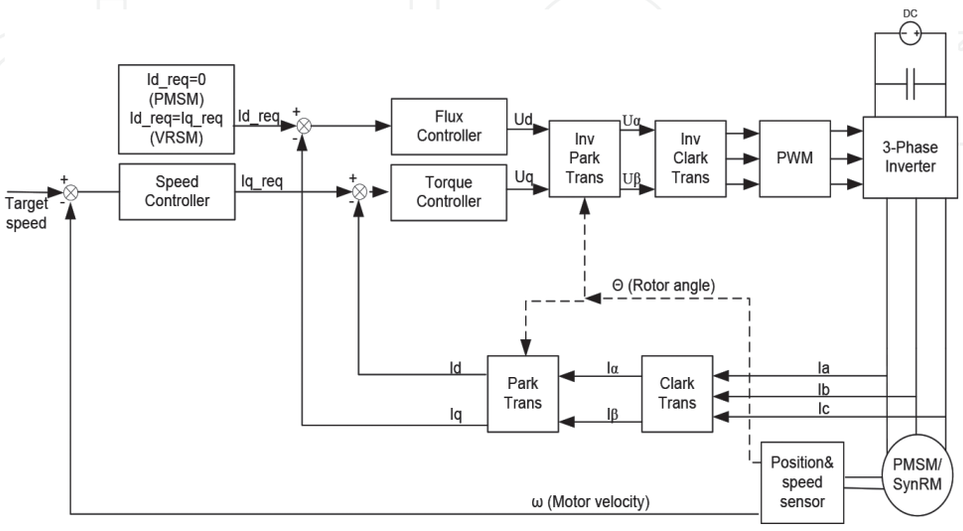

Figure 7. Block diagram of vector control system for PMSM and SynRM.

http://dx.doi.org/10.5772/intechopen.68861

$$I_{d\text{imposed}} = I_{q\text{imposed}} \cdot \frac{\cos(\theta)}{\sin(\theta)} \quad (4)$$

For the ideal machine, θ is in the range 0–90° and gives best performance at 45°. For a real machine, it has to be computed by varying its value and observing the performance of the machine for each angle step.

3. Simulation of a hybrid electric vehicle with the ISAB system

In order to study the electrical machines in ISAB applications, the electric drive model can be introduced and simulated in the Advanced Modelling Environment for performing Simulation (AMESim). AMESim is a multi-domain simulation software for the modelling and analysis of one-dimensional (1D) systems. In this program, each component or physical phenomenon is described by differential equations, type formulation in which the major variable is the time [31]. This approach is different from the partial derivate equations formulation, which formalizes the notion of the distribution of system properties in space. The representation of a dynamic system starting from the notion of "multiport" consists of highlighting the energy exchanges between a component and its environment through the connecting ports. The connection of two or more components through the port allows port exchange power (electrical, mechanical, etc.) according to the adopted sign convention.

For automotive applications, the program comprises discrete components of the ICE, gearbox, control system, electric loads, electrical machine and power inverter, connected together to form a global model of a hybrid electric vehicle.

The geometrical and electrical parameters of electrical machine considered for ISAB (SynRM) and BSAB (PMSMOR) application are presented in **Table 1**. The configuration of PMSMOR is a three-phase machine with 36 slots and 15 poles, and the SynRM topology is a three-phase machine with 27 slots and 4 poles. The dimension of PMSMOR has been imposed according to Ref. [32] (data chosen for belt brushless alternator).

The simulation of the BSAB and ISAB is carried out on a New European Driving Cycle (NEDC). A driving cycle is a series of points defining a speed profile that the studied vehicle must follow [33]. The defined speed profile simulates most common operating modes of an automobile (frequent acceleration and deceleration, load variations and speed variations) and corresponds to both urban and extra-urban environments. The parameters and the profile of NEDC are presented in **Table 2** and **Figure 8**, respectively.

The model takes into account the most complex thermodynamic phenomena occurring in a heat engine. In the initial implementation, the starter and alternator were a DC permanent magnets machine and the Lundell generator, respectively. The model has been replaced by the studied model and is shown earlier (PMSMOR/SynR). The motors are powered from a battery through the converter DC/DC that will operate in this case as a boost converter.

The evaluation of the performance of PMSMOR and SynRM was started from a demonstration model in AMESim of a compact car category (see **Figures 9** and **10**) with a compression-ignition

Parameter	PMSMOR	SynRM
Output power (W)	6500	10,000
Rated speed (rpm)	400	800
Phase voltage (V)	72	100
Number of phases (–)	3	3
Number of pole pairs (–)	15	2
Number of slots	39	30
Stator outer diameter (mm)	176	260
Stack length (mm)	150	150
Rotor outer diameter (mm)	210	210
Tooth width (mm)	5	6
Permanent magnet height (mm)	8	–
Residual flux density—NdFeB-N48 (T)	1.4	–
Coercive force—NdFeB-N48 (kA/m)	796	–
Stator and rotor (only for SynRM) lamination type	M270-35A	
Rated current (A)	72	72
Current density (A/mm^2)	7	6
Iron losses (W)	212	623
Torque (N m)	150	150
Power factor	0.9	0.85
Efficiency (%)	90	87
Saliency ratio	–	4.1

Table 1. Geometrical and electrical parameters of PMSMOR and SynRM.

Time (s)	Distance (km)	Max speed (km/h)	Average speed (km/h)	Max acceleration (m/s^2)	Max deceleration (m/s^2)	Idle functioning (s)	Stops
1184	10.93	120	33.21	1.06	-1.39	298	12

Table 2. NEDC parameters.

combustion engine. The imposed weight of the vehicle was 1200 kg (usually between 1134 and 1360 kg, according to Ref. [34]) without any extra weight or passengers.

In order to have comparative results regarding the fuel consumption, in the first simulation, the conventional vehicle functioning during the NEDC cycle was tested. In the next simulations,

http://dx.doi.org/10.5772/intechopen.68861

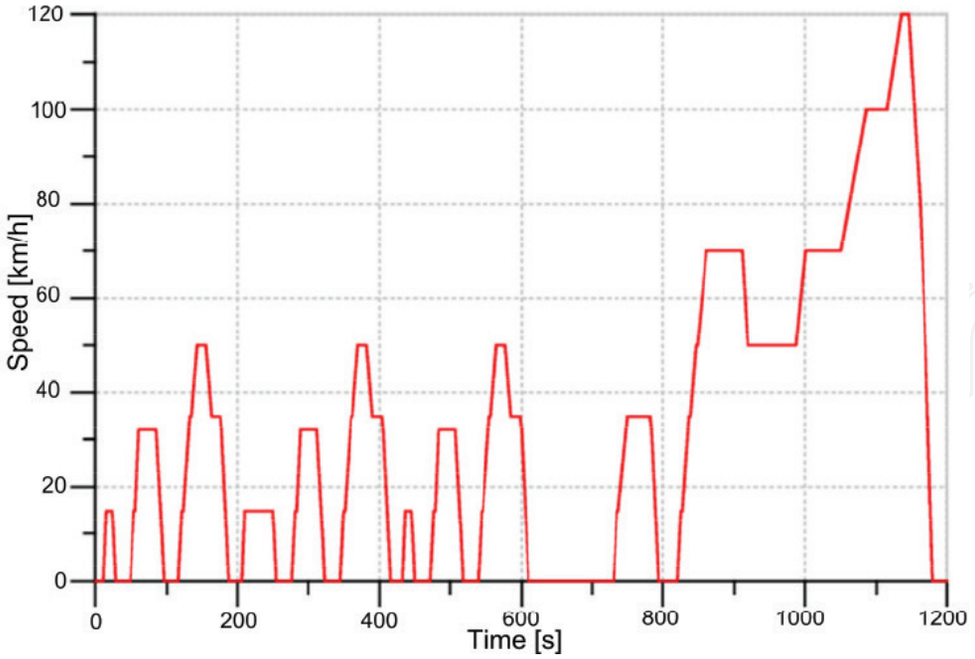

Figure 8. NEDC profile.

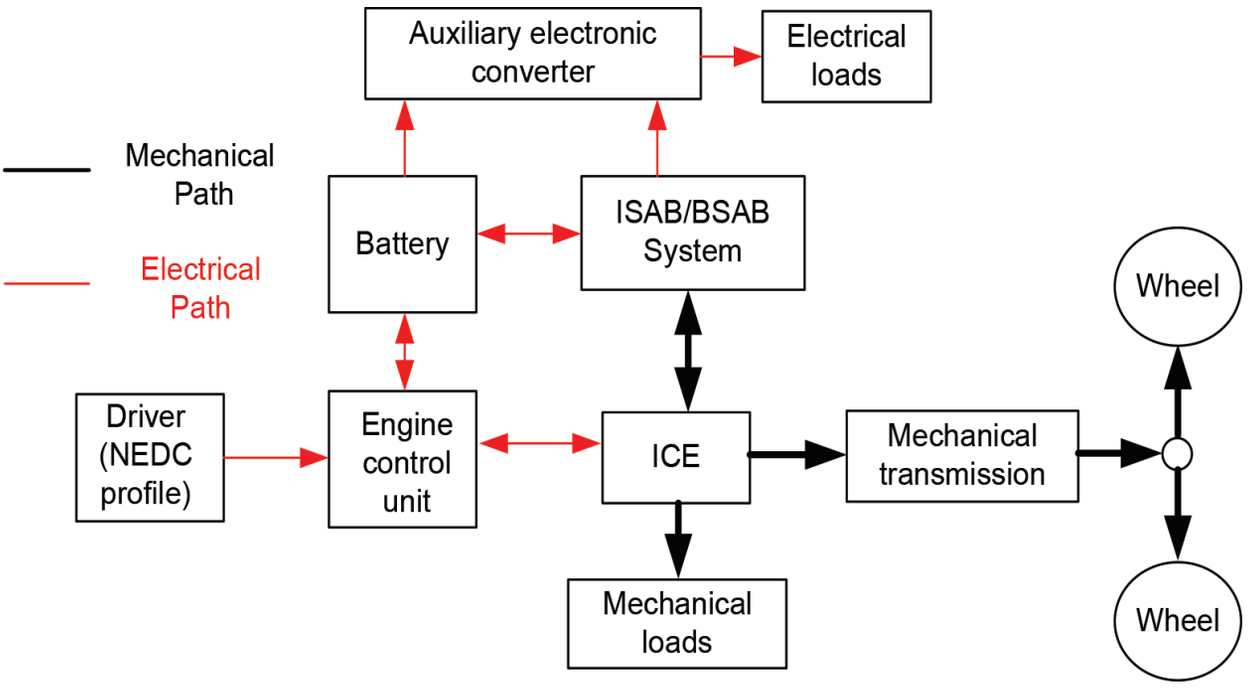

Figure 9. Structural diagram of the vehicle.

the ISAB regime with considered electrical machines was established. The behaviour of the starter and alternator in the vehicle model was supposed to be the same as in a conventional car. For the booster regime, a set-up to help ICE for 15 min/h was added and this works in the booster regime only when the battery was fully charged (up to 95%). The time limit for each

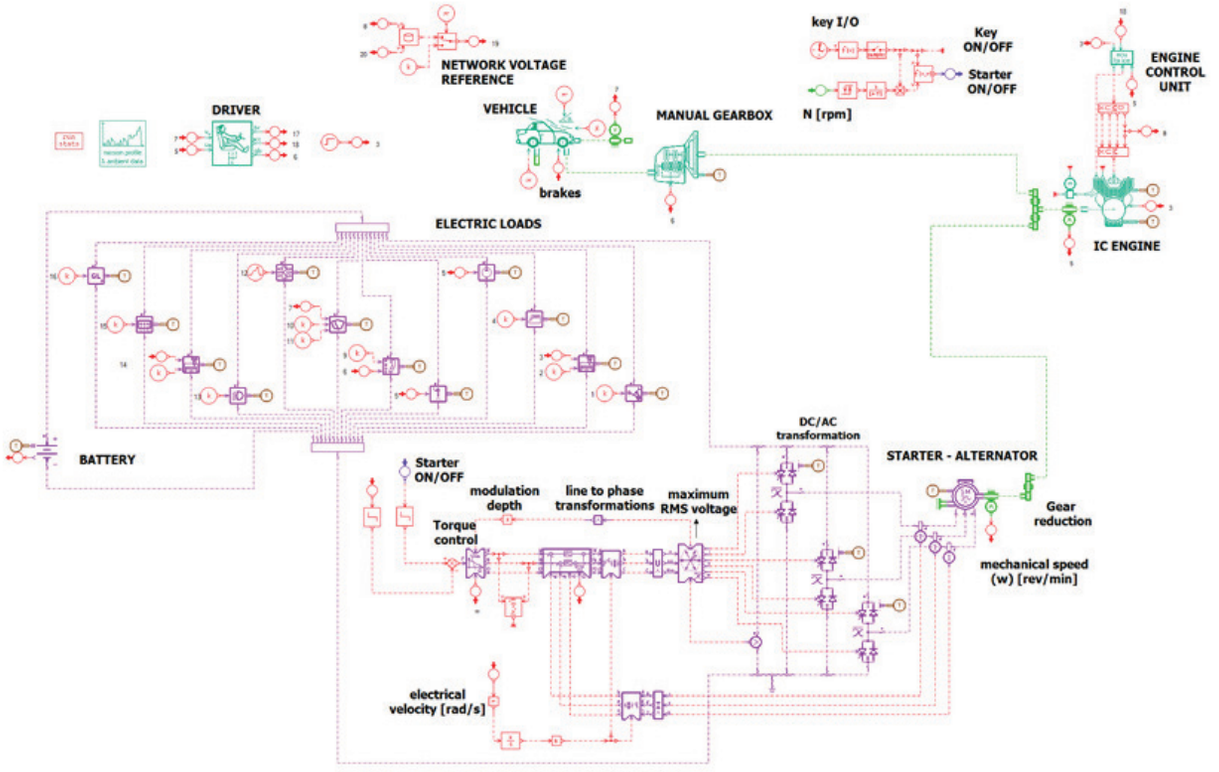

Figure 10. Vehicle model [35].

booster regime was set at 2 min in order to avoid the complete discharging of the battery (but no less than 20%). The parameters of the ICE considered are presented in **Table 3**.

The control of the electrical machines in the starter operating mode involves a maximum torque value (150 N m) until the ICE reaches 350 rpm. Torque command is provided by a bi-positional regulator with hysteresis. It is active when the command of ICE is active and its speed is less than 200 rpm, and it is off when the speed exceeds 400 rpm. When the ICE speed exceeds 300 rpm, the process of fuel injection into the cylinders starts and the ICE accelerates to idle speed. By applying the necessary torque to start the ICE, this is accelerated rapidly at the speed of 400 rpm in about 0.35 s.

When ICE exceeds the speed of 400 rpm, the bi-positional controller becomes inactive and the combustion engine continues to spin out due to its inertia. If the pistons do not reach the maximum compression point, they will not be able to inject fuel to start the combustion process; consequently, the speed drops below 200 rpm and now the controller output is active. Therefore, the starter is controlled again and the combustion engine is brought to a speed of 400

Type	Turbo diesel	Compression ratio	2:1
Number of cylinders	4	Maximum torque	365 N m at 2000 rpm
Cubic capacity	1994 cm^3	Maximum power	120 kW at 3750 rpm

Table 3. ICE parameters.

http://dx.doi.org/10.5772/intechopen.68861

rpm. At the start of the combustion engine process, ICE is accelerated to the idle speed, where it is maintained by the electronic control unit. The entire process of starting the engine (in normal condition), from the beginning until stable operation at idle speed, lasts 0.8 s. In the winter, this process may take 1.5 s. The speed profile of starting the ICE is presented in **Figure 11**.

For the alternator mode, the nominal value of the electrical loads is considered in the model. Some electrical loads are intermittently connected (fan, electrical window, heating systems, etc.). Other loads are dependent on ICE speed (fuel pump and injectors) or the speed of the vehicle.

When the entire driving cycle is considered, the fuel consumption in the vehicle is reduced to 878.63 ml for the BSAB system and 941 ml for the ISAB system. These values represent a fuel economy of around 16% for BSAB and 17.3% for ISAB of total consumption compared with a classical vehicle with a dedicated alternator and starter (without booster option) system. The difference in fuel consumption is due to the value of nominal power of electrical machines (see **Table 1**). But, the performances of SynRM are limited by the battery (which uses 75 Ah) capacities. If it uses a stronger battery, the total fuel economy can be increased with 2 or 4% (especially due to the booster mode).

In the mechanical evaluation of electrical machines for automotive applications, the variation of electromagnetic torque is one of the most important parameters, because this variation (torque ripple) can become a source of noise and vibration in vehicles. Thus, for a better visualization of the torque profile of PMSMOR and SynRM, a new scenario for all three regimes was considered. For better comparative results (variation of axis torque) between IASB and BSAB, the BSAB system is taken into account through directly coupling (using ratio 1:1 between ICE and BSAB speed) at ICE. The starter and generator regime has been set for 1.5 and 20 s, respectively. The variation of the axis torque in the generator mode has been obtained by intermittent connection of the electrical loads (lights, HVAC, media, etc.). For the booster mode, the speed of the vehicle is increased from 70 to 120 km/h in 17 s, necessary to overtake other vehicles. In this case, the battery is considered fully charged.

Figures 12 and **13** show the variation of the axis torque versus time for all operating modes, respectively. Due to the proper windings-slot combination, the torque ripple values are below

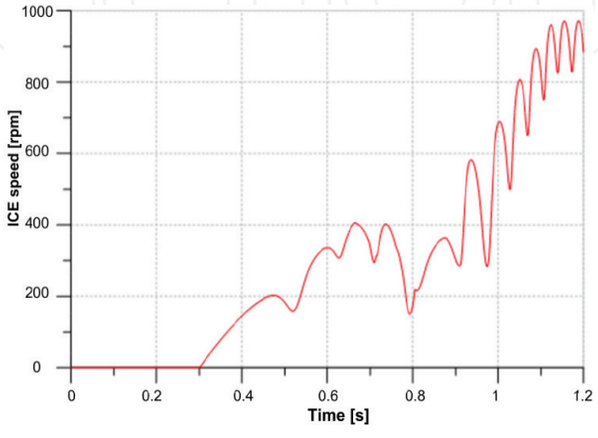

Figure 11. Speed profile at starting ICE.

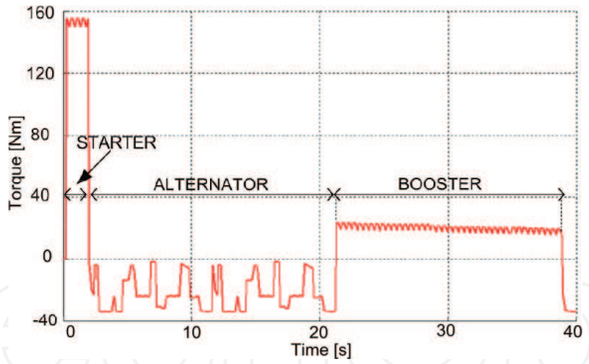

Figure 12. BSAB torque profile.

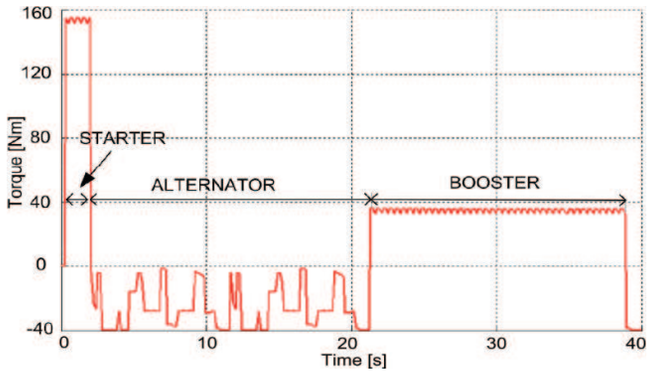

Figure 13. ISAB torque profile.

10%. In fact, the ratio of the torque ripple is 7.1% for PMSMOR and 6.2% for SynRM. In the booster mode, the rated torque value of the 10 kW SynRM machine used for ISAB is obviously bigger than that of the 6.5 kW PMSMOR.

4. Conclusions

The chapter presents the main steps to be followed in the development of a specific electric drive system dedicated to automotive domain, such as integrated starter-alternator-booster applications. Replacing the starter and alternator in a conventional vehicle with extended possibility to work in booster mode represents the first step of vehicles' hybridization, called *Mild-HEV*. In this way, two variants in mounting the ISAB had been identified in the literature: one, directly driven generic called ISAB and another belt-driven called BSAB. In this chapter, the approach contains the major elements that need to be discussed for two type of electrical machine (PMSMOR and SynRM) suitable for BSAB and ISAB, respectively. The general design procedure is presented for these two electrical machines by taking into account the typical constraints of the applications and the behaviour of the machine (thermal, structural, and noise, vibrations and harshness particularities). Also, the control aspects of both electrical machines are presented.

In order to demonstrate the capability of this vehicle hybridization method, two electrical machines have been designed and the equations model was developed and implemented in the general 1D model of conventional vehicle performed in AMESim software. The influence of fuel consumption on the entire drive cycling (NEDC) was investigated. Based on the obtained results, the ISAB system gives a greater value of the reduction of fuel consumption, but the coupling of the electrical machine directly to the crankshaft involves complicated manufacturing techniques (higher cost) compared with the BSAB system procedure.

Acknowledgements

This work was supported by a grant of Strengthening the Research potential of CAREESD in the field of Electromechanical Systems and Power Electronics for Sustainable Applications, ESPESA, 692224/2015 H2020 TWINNing-2015 and ALNEMAD (PCCA 181/2012).

Author details

Florin-Nicolae Jurca* and Mircea Ruba

*Address all correspondence to: florin.jurca@emd.utcluj.ro

Department of Electrical Machines and Drives, Technical University of Cluj-Napoca, Cluj-Napoca, Romania

References

[1] Andreescu G-D, Coman CE. Integrated starter-alternator control system for automotive. In: Proceedings of the International Symposium on Computational Intelligence and Informatics (CINTI '13), 19-21 Nov. 2013, Budapest, Hungary, p. 339-343, Publisher: IEEE.

[2] Mirahki H, Moallem M, Rahimi SA. Design optimization of IPMSM for 42 V integrated starter alternator using lumped parameter model and genetic algorithms. IEEE Transactions on Magnetics. 2014, Vol: 5, NO: 3, pp. 1-6, DOI: 10.1109/TMAG.2013.2285358

[3] Rizoug N, Barbedette B, Sadoun R, Feld G, Starter-alternator propel the vehicle through a hybrid supply: Battery and supercapacitors. In: Proceedings of the Twenty-Seventh Annual IEEE Applied Power Electgronics Conference and Exposition (APEC'12); 5-8 February 2012; Orlando, Florida, USA. pp. 2583-2589, Publisher: IEEE.

[4] Mirahki H, Moallem M. Design improvement of Interior Permanent Magnet synchronous machine for Integrated Starter Alternator application. In: Proceedings of the International Electric Machines & Drives Conference (IEMDC'13); 12-15 May; Chicago, Illinois, USA. pp. 382-385, Publisher: IEEE.

[5] Parsa L, Goodarzi A, Toliyat HA. Five-phase interior permanent magnet motor for hybrid electric vehicle application. In: Proceedings of the IEEE Conference of Vehicle Power and Propulsion (VPPC' 05); 7-9 September 2005; Chicago, Illinois, USA. pp. 631-637, Publisher: IEEE.

[6] Ivankovic R, Cros J, Kakhki MT, Martins CA, Viarouge P. Power electronic solutions to improve the performance of Lundell automotive alternators. In: Carmo J, editors. New Advances in Vehicular Technology and Automotive Engineering. Rijeka, InTech; 2012. DOI:10.5772/48459

[7] Jurca FN, Ruba M, Martis C. Analysis of permanent magnet synchronous machine for integrated starter-alternator-booster applications. In: Proceedings of the 2015 International Conference on Electrical Drives and Power Electronics (EDPE'15); 21-23 September 2015; High Tatras, Slovakia. pp. 272-276, Publisher: IEEE.

[8] Hagstedt D. Comparison of different electrical machines for belt driven alternator starters [thesis]. Lund: Department of Measurement Technology and Industrial Electrical Engineering, Lund University; 2013

[9] Frost & Sullivan, Strategic Analysis of Electric Motor Technologies for Electric and Hybrid Vehicles in Europe. http://www.automotive.frost.com [Accessed: 6-January 2017]

[10] Bae BH, Sul S.K, Practical design criteria of interior permanent magnet synchronous motor for 42V integrated starter-generator, In: Proceedings of the IEEE International Electric Machines and Drives Conference (IEMDC' 03); 1-4 June 2003; Madison, Wisconsin, USA. pp. 656-662

[11] Schofield N, Long S, Generator operation of a switched reluctance Starter/Generator at extended speeds. IEEE Transactions on Vehicular Technology. 2009;**58**:48-56. DOI: 10.1109/TVT.2008.924981

[12] Rehman H. An integrated starter-alternator and low-cost high performance drive for vehicular applications. IEEE Transactions on Vehicular Technology. 2008;**57**:1454-1465. DOI: 10.1109/TVT.2007.909255

[13] Krishnan R. Permanent Magnet Synchronous and Brushless DC Motor Drives. Boca Raton, FL: CRC Press/Taylor & Francis; 2010. p. 611

[14] Gieras JF, Permanent Magnet Motor Technology: Design and Applications. 3rd ed. Boca Raton, FL: CRC Press/Taylor & Francis; 2011. p. 608

[15] Lei G, Zhu J, Guo Y. Multidisciplinary Design Optimization Methods for Electrical Machines and Drive System. Berlin/Heidelberg:/Springer-Verlag; 2016. p. 251

[16] Mutluer M, Bilgin O. Comparison of stochastic optimization methods for design optimization of permanent magnet synchronous motor. Neural Computing and Applications. 2012;**21**(8):2049-2056

[17] Deb A, Gupta B, Roy J. Performance comparison of differential evolution, genetic algorithm and particle swarm optimization in impedance matching of aperture coupled microstrip antennas. In: 11th Mediterranean Microwave Symposium (MMS); September 2011; Tunisia. pp. 17-20, Publisher: IEEE.

[18] Stipetic S, Miebach W, Zarko D. Optimization in design of electric machines: Methodology and workflow; In: Proceedings of the ACEMP-OPTIM-ELECTREMOTION join conference; 2-4 September 2015; Side, Turkey. pp. 1-8, Publisher: IEEE.

[19] Malan J, Kamper MJ. Performance of a hybrid electric vehicle using reluctance. IEEE Transaction on Industry Applications. 2001;**37**:1319-1324. DOI: 10.1109/28.952507

[20] Jurca FN, Ruba M, Martis C. Design and control of synchronous reluctances motors for electric traction vehicle. In: Proceedings of the 2016 International Symposium on Power Electronics, Electrical Drives, Automation and Motion (SPEDAM '16); 22-24 June 2016; Anacapri, Italy. pp. 1144-1148, Publisher: IEEE.

[21] Wu H, Lin Q, You L. An investigation of the synchronous motor. In: Proceedings of the Fifth International Conference on Electrical Machines and Systems (ICEMs' 01); 18-20 August 2001; Shenyang, China. pp. 148-151, Publisher: IEEE.

[22] Wang K, Zhu ZQ, Ombach G, Koch M, Zhang S, Xu J, Optimal slot/pole and flux-barrier layer number combinations for synchronous reluctance machines. In: Proceedings of the Eight International Conference and Exhibition on Ecological for Synchronous Reluctance Machines (EVER' 13); 27-30 March 2013; Monte Carlo. pp. 1-8, Publisher: IEEE.

[23] Fukami T, Momiyama M, Shima K, Hanaoka R, Takata S. Steady-state analysis of a dual-winding reluctance generator with a multiple-barrier rotor. IEEE Transactions on Energy Conversion. 2008;**23**:492-498. DOI: 0.1109/TEC.2008.918656

[24] Bianchi N, Blognani S, Carraro E, Castiello M, Fornasiero E, Electric vehicle traction based on synchronous reluctance motors. IEEE Transaction on Industry Applications. 2016;**52**:4762-4769. DOI: 10.1109/TIA.2016.2599850

[25] Ehsani M, Gao Y, Gay S. Characterization of electric motor drive for traction applications. In: Proceedings of the IEEE 29th Annual Conference of the Industrial Electronics Society (IECON'03); Roanoke, USA. pp. 891-896

[26] Hangiu R.P, Martis C. A Review of Automotive Integrated Starter Alternators, The Scientific Bulletin of Electrical Engineering Faculty, 2012, p.1-6

[27] Yamanaka M, Koizumi H. A bi-directional Z-source inverter for electric vehicles. In: Proceedings of the International Conference on Power Electronics and Drive Systems (PEDS'09); 2-5 November 2009; Taipei, Taiwan. pp. 574-578, Publisher: IEEE.

[28] Cai W. Comparison and review of electric machines for integrated starter alternator applications. In: Proceedings of the 39th IAS Annual Meeting; 3-7 October 2004; Seattle, USA. pp. 386-393, Publisher: IEEE.

[29] Novotny DW, Lipo TA. Vector Control and Dynamics of AC Drives. Oxford: Clarendon Press; 1999. p. 464

[30] Ruba M, Jurca FN, Martis C. Analysis of Synchronous Reluctance Machine for Light Electric Vehicle Applications, In: Proceedings of the 2016 International Symposium on Power Electronics, Electrical Drives, Automation and Motion (SPEDAM '16), 22-24 June 2016, Anacapri, Italy, pp. 1138-1143

[31] AMESim® User's Guides [internet].https://www.plm.automation.siemens.com/en/products/lms/imagine-lab/amesim. Accessed: 2017-02-27.

[32] Electrical Specifications & Selection Guide Starter and Alternators-Delco Remy. 2008 [internet]. http://www.dieselusa.com/productinfo/Delco%20Electrical%20Specs%20and%20Seletion%20Guide.pdf. Accessed: 2016-08-12.

[33] Zhang X, Chris M. Vehicle Power Management. Berlin/Heidelberg: Springer-Verlag; 2011. p. 346

[34] Code of Federal Regulations, Title 40, Protection of Environment, Parts 425 to 699. US: Office of the Federal Register; 2010

[35] Jurca FN, Martis C, Hangiu RP. Design and performance analysis of an integrated starter-alternator for hybrid electric vehicles. In: Proceedings of the Interdisciplinary research in engineering: Steps towards breakthrough innovation for sustainable development. Advanced Engineering Forum. 2013;**8-9**:453-460